

Nonlinear dynamic analysis of reinforced concrete shell structures

T.-H. Kim¹, J.-G. Park², J.-H. Choi³ and H.M. Shin^{2*}

¹Civil Engineering Research Team, Daewoo Institute of Construction Technology,
60 Songjuk-dong, Jangan-gu, Suwon, Gyeonggi-do 440-210, Korea

²Department of Civil and Environmental Engineering, Sungkyunkwan University,
300 Cheoncheon-dong, Jangan-gu, Suwon, Gyeonggi-do 440-746, Korea

³Department of Civil Engineering, Hankyong National University, 67 Sukjong-dong,
Ansung, Gyeonggi-do 456-749, Korea

(Received July 14, 2008, Accepted December 23, 2009)

Abstract. In this paper, a nonlinear finite element procedure is presented for the dynamic analysis of reinforced concrete shell structures. A computer program, named RCAHEST (Reinforced Concrete Analysis in Higher Evaluation System Technology), was used. A 4-node flat shell element with drilling rotational stiffness was used for spatial discretization. The layered approach was used to discretize the behavior of concrete and reinforcement in the thickness direction. Material nonlinearity was taken into account by using tensile, compressive and shear models of cracked concrete and a model of reinforcing steel. The smeared crack approach was incorporated. The low-cycle fatigue of both concrete and reinforcing bars was also considered to predict a reliable dynamic behavior. The solution to the dynamic response of reinforced concrete shell structures was obtained by numerical integration of the nonlinear equations of motion using Hilber-Hughes-Taylor (HHT) algorithm. The proposed numerical method for the nonlinear dynamic analysis of reinforced concrete shell structures was verified by comparison of its results with reliable experimental and analytical results.

Keywords: reinforced concrete; shell structures; layered approach; material nonlinearity; low-cycle fatigue; hilber-hughes-taylor algorithm.

1. Introduction

Many large-scale reinforced concrete shell structures, such as underground tanks, nuclear power containers, huge silos, cooling towers and offshore structures, have been built in active seismic zones. Therefore, these structures have to be designed for extraordinary dynamic loads such as extreme accidental internal loads and external catastrophic loads.

Due to the complex geometry, boundary conditions, and highly nonlinear behavior of these structures, conventional analysis cannot predict their nonlinear behaviors satisfactorily. Nonlinear finite element analysis is a more efficient and effective tool to check the performance of these structures in accordance with the performance-based design method.

*Corresponding author, Professor, E-mail: hmshin@skku.ac.kr

Much research has been done to develop suitable finite element analysis for reinforced concrete shell structures subjected to dynamic loading (ASCE 1993, ACI 2001, ASCE 2001, Semblat *et al.* 2004). The results of a nonlinear dynamic analysis and therefore the design of structural members can be influenced substantially when nonlinear material behavior of reinforced concrete is considered up to a defined point of dynamic failure.

In the present study, the nonlinear material model for reinforced concrete was developed to address material nonlinearity by incorporating tensile, compressive and shear models for cracked concrete, and a model for the reinforcing steel, which uses the smeared crack approach. The low-cycle fatigue model of concrete and that of reinforcing bars under dynamic load were newly incorporated into the material model for RCAHEST to predict the dynamic behavior of reinforced concrete shell structures. These models were developed to express dynamic behavior by proper theoretical representation of the material parameters.

The primary objective of this study is to develop a new finite element formulation for the nonlinear dynamic analysis of shell structures. To analyze reinforced concrete shell structures with highly nonlinear behavior, the layer method was used, assuming that several thin plane stress elements are layered in the direction of thickness. The cross section of the reinforced concrete was divided into concrete and steel layers. Each layer consisted of four-node flat shell elements. The flat shell element was developed by combining a membrane element with drilling degree of freedom and a plate-bending element. Thus, the developed element possesses six degrees of freedom (DOF) per node, so it can be easily connected to other types of finite elements that have with 6-DOFs per node, a three-dimensional beam-column element, etc., and be a much improved, more robust dynamic analysis procedure than the general shell element with five degrees of freedom.

An additional objective was to create a finite element model that could be used as an analysis tool for a wide range of practical engineering applications.

2. Nonlinear finite element analysis program RCAHEST

RCAHEST is a nonlinear finite element analysis program for analyzing reinforced concrete structures. The program was developed by Kim and Shin (2001), at the Department of Civil and Environmental Engineering, Sungkyunkwan University. This program has been used to analyze various concrete structures under various loading conditions.

In the present study, authors attempt to incorporate such reinforced concrete shell element into RCAHEST, and modify the material models so that they could be made suitable for the dynamic analysis.

2.1 Reinforced concrete shell element

The element developed for the nonlinear analysis of reinforced concrete shell structures was a four-node quadrilateral flat-shell element with 6-DOFs (Kim *et al.* 2002). The sixth DOF was obtained by combining a membrane element with a normal rotation, θ_z , the so-called drilling degree of freedom, and a discrete Kirchhoff plate element.

Flat shell finite elements may be formulated by using a variational formulation that includes an independent rotation field for the drilling degree of freedom. These modeling assumptions are shown in Fig. 1. The element had to be based on a three-dimensional formulation. To analyze reinforced concrete shell structures with nonlinear behavior, the layer method was used, assuming that several

thin plane stress elements are layered in the direction of thickness. In the layered element formulation, the shell was divided into several paneled layers and two-dimensional constitutive models were applied to take into account material nonlinearities.

Fig. 2 illustrates the layered element and forces acting on the shells. Integration through the thickness of element was achieved through layered-element formulation. In the depth of its mid-surface, one-integration point was used for each layer of the panel. Each layer was classified as either a plain concrete layer or a reinforced concrete layer, where the reinforcing bars were smeared in the layer, as shown in Fig. 2.

2.2 Nonlinear material model for reinforced concrete

The nonlinear material model for the reinforced concrete was composed of models to characterize the behavior of the concrete, in addition to a model for characterizing the reinforcing bars. Models for concrete may be divided into models for uncracked concrete and cracked concrete. The basic model adopted for crack representation was a non-orthogonal fixed-crack method of the smeared crack concept, which is widely known to be a robust model for crack representation. This approach is practical for cyclic loads where the load history needs to be recorded. This section includes a summary of the material models used in the analysis. A full description of the nonlinear material model for reinforced concrete is given by the authors (Kim *et al.* 2002, Kim *et al.* 2003, Kim *et al.*

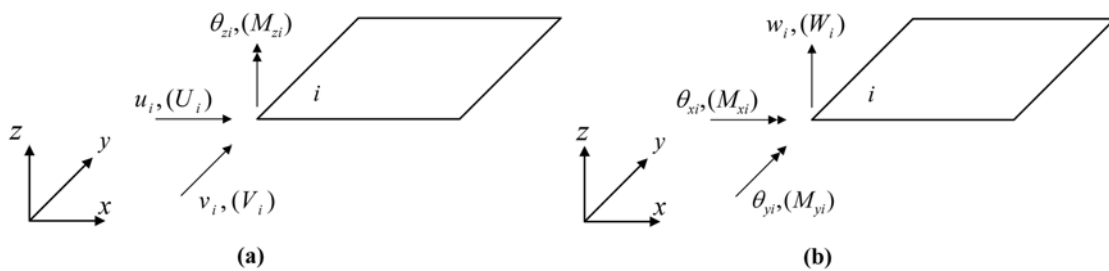


Fig. 1 A flat shell element subjected to plane membrane and bending action (a) plane membrane actions and deformations, (b) bending actions and deformations

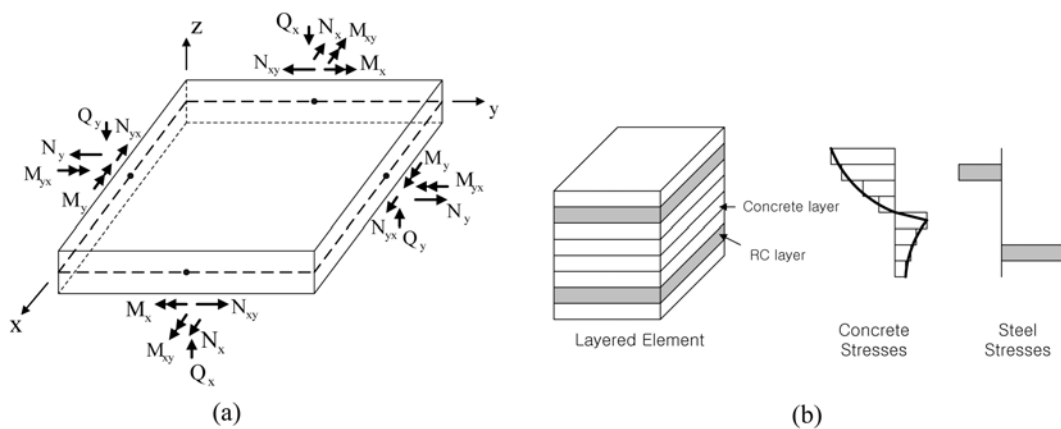


Fig. 2 Shell element (a) forces acting on RC shells, (b) layered element

2005, Kim *et al.* 2006, Kim *et al.* 2008).

2.2.1 Model for uncracked and cracked concrete

The widely used elasto-plastic and fracture model for the biaxial state of stress proposed by Maekawa and Okamura (1983) was used as the constitutive equation for the uncracked concrete. For uncracked concrete, the nonlinearity, anisotropy, and strain softening effects were expressed independently of its loading history.

After concrete cracks, the behavior becomes anisotropic in the crack direction. The stress-strain relations are modeled by being decomposed in directions parallel to, along and normal to cracks, respectively. Thus, the constitutive law adopted for the cracked concrete is formed from tension stiffening, compression stiffness and shear transfer models (see Fig. 3).

Cracked concrete may resist a certain amount of tensile stress normal to the cracked plane because of the bond effect between the concrete and the reinforcing bars. A refined tension stiffening model is obtained by transforming the tensile stresses of concrete into the component normal to the crack, and improved accuracy is expected, especially when the reinforcing ratios in orthogonal directions are significantly different and when the reinforcing bars are distributed only in one direction. For the tension stiffening model for unloading and reloading, the model proposed by Shima *et al.* (1987) was basically used.

A modified elasto-plastic fracture model was used to describe the compressive behavior of the concrete struts in between cracks in the direction of the crack plane. The model describes the degradation in compressive stiffness with a modified fracture parameter expressed in terms of the strain perpendicular to the crack plane. The cyclic load causes damage to the inner concrete and energy is dissipated during the unloading and reloading processes. This behavior is considered in the model with the modification of the stress-strain curve at unloading to an experimentally fitted quadratic curve as shown in Fig. 4.

The shear transfer model based on the contact surface density function (Li *et al.* 1989) was used

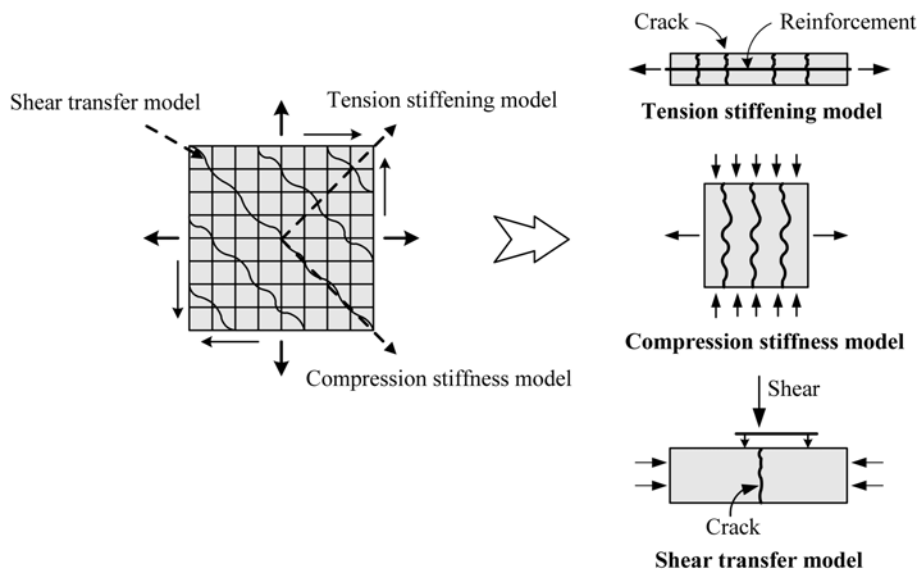


Fig. 3 Construction of cracked concrete model

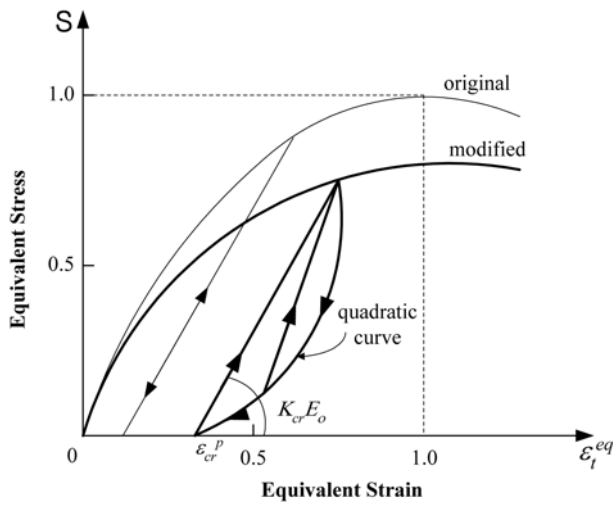


Fig. 4 Equivalent stress-equivalent strain relationship for concrete during unloading and reloading

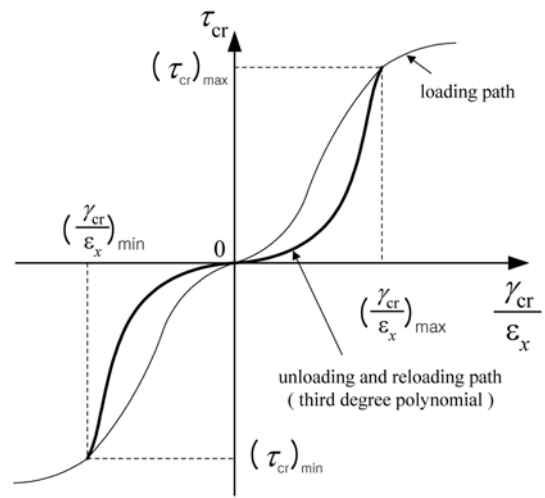


Fig. 5 Shear transfer model for concrete

to consider the effect of shear stress transfer due to the aggregate interlock at the crack surface. The contact surface was assumed to respond elasto-plastically. The model can be applied to any arbitrary loading history. For the shear transfer model for unloading and reloading, the model modified by the authors (Kim *et al.* 2002) was used (see Fig. 5).

2.2.2 Model for the reinforcing bars in concrete

The stress acting on the reinforcing bar embedded in concrete is not uniform and reaches a maximum value at locations where the bar is exposed to a crack plane. The constitutive equations for the bare bar may be used if the stress-strain relation remains in the elastic range. The post-yield

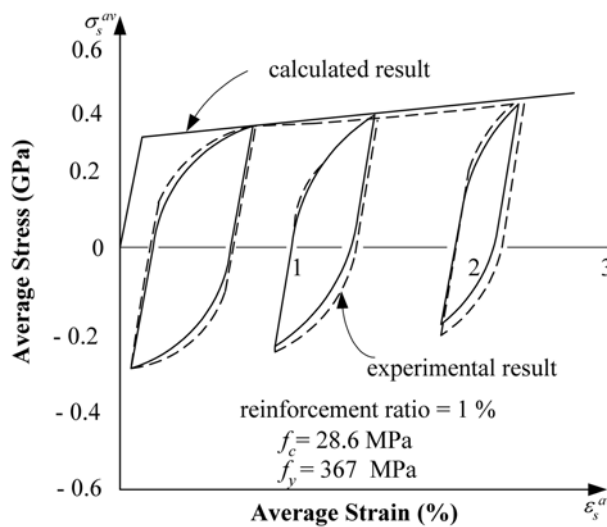


Fig. 6 Reinforcement model for reversed cyclic loading

constitutive law for the reinforcing bar in concrete considers the bond characteristics. The bilinear model was used (Kim *et al.* 2002).

Kato's model (1979) for the bare bar under the reversed cyclic loading and the assumption of cosinusoidal stress distribution were used to derive the mechanical behavior of reinforcing bars in concrete under the reversed cyclic loading. A modified version of the model for the post-yield steel behavior for unloading and reloading branches is shown in Fig. 6.

For reinforcing bars under extreme compression, the lateral bar tends to buckle and this greatly affects the post peak behavior and member ductility. To account for the buckling, the average stress-strain behavior of reinforcing bars after concrete crushing is assumed to be linearly descending until the 20% of the average steel stress. This relation has been derived from a parametric study using finite element analysis (Kim *et al.* 2005).

2.3 Modeling of the low-cycle fatigue behavior

When a structure is subjected to dynamic loads, especially seismic loads, the behavior of the structural material can be significantly different from that when the structure is subjected to static loads. In general, earthquake excitation belongs to the category of so-called 'low-cycle fatigue'. The principal characteristics of the loading history that the structure is subjected to during an earthquake are a high rate of loading and a number of load cycles with varying amplitudes and periods. Thus, any numerical model for reinforced concrete intended for transient analysis should be rate and loading history dependent. This study corrects the nonlinear material model by accounting for the above effects (Kim *et al.* 2005).

2.3.1 Fatigue model of reinforcing bars

Research has proven that plastic strain of reinforcing bars is an important variable of low-cycle fatigue. This study applied the Coffin-Manson's equation (Mander *et al.* 1994) as follows

$$\varepsilon_{ap} = 0.0777(N_{2fo})^{-0.486} \quad (1)$$

where $\varepsilon_{ap} = \Delta\varepsilon_p/2$; $\Delta\varepsilon_p = (\varepsilon_p)_{\max} - (\varepsilon_p)_{\min}$; N_{2fo} = number of complete cycles to failure for original model; $(\varepsilon_p)_{\max}$ = maximum strain by number of cycles; and $(\varepsilon_p)_{\min}$ = minimum strain by number of cycles.

Despite the reliability of Eq. (1), the N_{2fo} needs to be modified for application to reinforced concrete, because Eq. (1) was derived from the bare bar test. From the numerical test results, N_{2fo} is yielded the following relationship.

$$N_{2fr} = k_r N_{2fo} \quad (2)$$

where N_{2fr} = number of complete cycles to failure for reinforcing bars; k_r = modification factor for reinforcing bars ($= 1.5s_k$); $s_k = f'_{cc}/f'_{co}$; f'_{cc} = confined concrete compressive strength; and f'_{co} = unconfined concrete compressive strength.

Following Miner's rule (1945), the accumulated fatigue damage of reinforcing bars (AD_r) can be derived.

$$AD_r = \sum_{i=1}^n \frac{1}{(N_{2fr})_i} \quad (3)$$

2.3.2 Fatigue model of concrete

One of the important characteristics of the fatigue process is the strength degradation under cyclic loading. Experimental results show that the degradation is a function of the number of load repetitions, as well as the stress range of the load cycles.

Kakuta *et al.*'s formula (1982) derived from plain concrete specimens tests was adopted for the fatigue model of concrete. The modifications are also performed to apply to the reinforced concrete. The first modification was to determine the number of cycles to failure by strains in the calculated Gauss integral calculus point instead of by stress in Kakuta *et al.*'s formula, and the other modification was to multiply a modification factor to apply to reinforced concrete

$$\log \frac{N_{2fc}}{k_c} = \begin{cases} \frac{1}{\beta} \left[1 - \frac{(\varepsilon_{co} - \varepsilon_{\min})^2 - (\varepsilon_{co} - \varepsilon_{\max})^2}{(\varepsilon_{co} - \varepsilon_{\min})} \right], & \varepsilon_{\max} < 0.7 \varepsilon_{co} \\ \frac{0.09 \varepsilon_{cu}}{\varepsilon_{cu} - 0.7 \varepsilon_{co}} \frac{1}{\beta} \frac{\varepsilon_{\max} - \varepsilon_{\min}}{\varepsilon_{cu} - \varepsilon_{\min}}, & \varepsilon_{\max} \geq 0.7 \varepsilon_{co} \end{cases} \quad (4)$$

where N_{2fc} = number of complete cycles to failure for concrete; k_c = modification factor for concrete (= 2.0 s_k); ε_{co} = strain of unconfined concrete at peak stress; ε_{\min} = cyclic minimum strain; ε_{\max} = cyclic maximum strain; ε_{cu} = compressive strain of confined concrete at failure; and β = material constant equal to 0.0588.

Miner's rule was also used to consider the accumulated fatigue damage of concrete.

3. Nonlinear dynamic analysis procedure

The Newmark's implicit integration method, together with the Hilber-Hughes-Taylor α -method, was adopted in the present implementation for the solution of the dynamic equilibrium equations (Taylor 2000).

Numerical damping cannot be introduced in the Newmark method without degrading the order of accuracy. Therefore, Hilber, Hughes, and Taylor introduced the α -method (Hughes 2000).

The Newmark algorithm can be altered by considering the residual in the momentum equation which is given by

$$R(t_{n+\alpha}) = F(t_{n+\alpha}) - P(u_{n+\alpha}, v_{n+\alpha}, a_{n+\alpha}) = 0 \quad (5)$$

where R = residual force vector; F = equivalent nodal force vector; P = equivalent internal force vector; $u_{n+\alpha}$ = displacement; $v_{n+\alpha}$ = velocity; and $a_{n+\alpha}$ = acceleration.

The displacement and velocity at the intermediate point are given by

$$u_{n+\alpha} = (1 - \alpha)u_n + \alpha u_{n+1} \quad (6)$$

$$v_{n+\alpha} = (1 - \alpha)v_n + \alpha v_{n+1} \quad (7)$$

In the above $t_{n+\alpha} = (1 - \alpha)t_n + \alpha t_{n+1}$. This algorithm is called the Hilber-Hughes-Taylor α -method or, for short, the HHT-method and has been proved extensively for linear problems have been done by Hughes (2000) for stability and dissipative properties. To reduce the properties to a single parameter, the relations is given by

$$\beta = \frac{(2-\alpha)^2}{4} \quad (8)$$

$$\gamma = \frac{3}{2} - \alpha \quad (9)$$

$$\frac{1}{2} \leq \alpha \leq 1.0 \quad (10)$$

In this study, default values are $\beta = 0.5$, $\gamma = 1$, and $\alpha = 0.5$. The definition of α is different than in the original paper (Hughes 2000).

Linearization of Eq. (5) gives the tangent matrix

$$K^* = \frac{1}{\beta \Delta t^2} M + \frac{\alpha \gamma}{\beta \Delta t} C + \alpha K \quad (11)$$

where M = mass matrix; C = tangent damping matrix; and K = tangent stiffness matrix.

The Newton-Raphson iteration scheme was used to carry out iterative corrections to the displacement increment to solve the nonlinear equations of equilibrium obtained by linearizing Eq. (5).

4. Numerical examples

The proposed structural element library RCAHEST is built around the finite element analysis program named FEAP, developed by Taylor (2000). FEAP is characterized by a modular architecture and by the facility that introduces the types of custom elements, input utilities, and custom strategies and procedures. The results from the analysis of three numerical examples are compared with existing analytical and experimental results to show the efficiency and reliability of the method.

4.1 Reinforced concrete plate subjected to a jet force

The program was validated by analyzing the benchmark problem of a reinforced concrete clamped slab subjected to a time varying jet force reported by Stangenberg (1974). The problem was analyzed by Stangenberg who used the finite difference method and an elasto-plastic material model. The details of plate geometry, steel reinforcement and time history of the jet force are shown in Fig. 7 and Fig. 8. The material properties used in the analysis are given Table 1.

For finite element analysis, the specimens were modeled using a mesh of eighty elements as shown in Fig. 9. Ten layers per element were used for the integration through the depth. For nonlinear problems of reinforced concrete structures, the ratio of the fundamental period of vibration to the time step of integration (Δt), i.e., $T/\Delta t$, should be between 20 and 30 to keep the computational errors within acceptable limits. The fundamental period of vibration (T) of the plate was 0.025 second. A time step of $\Delta t = 0.001$ second ($T/25$) with a total of 100 steps was used for time step integration. No damping was assumed.

The resulting mid-span deflection-time history for the plate is presented in Fig. 10, as well as the results given by Stangenberg (1974). The maximum deflection obtained in the current investigation was 8.5 mm at 0.0170 second. The value of maximum deflection reported by Stangenberg using the finite difference method was 8.1 mm at 0.0153 second. The difference between the values of

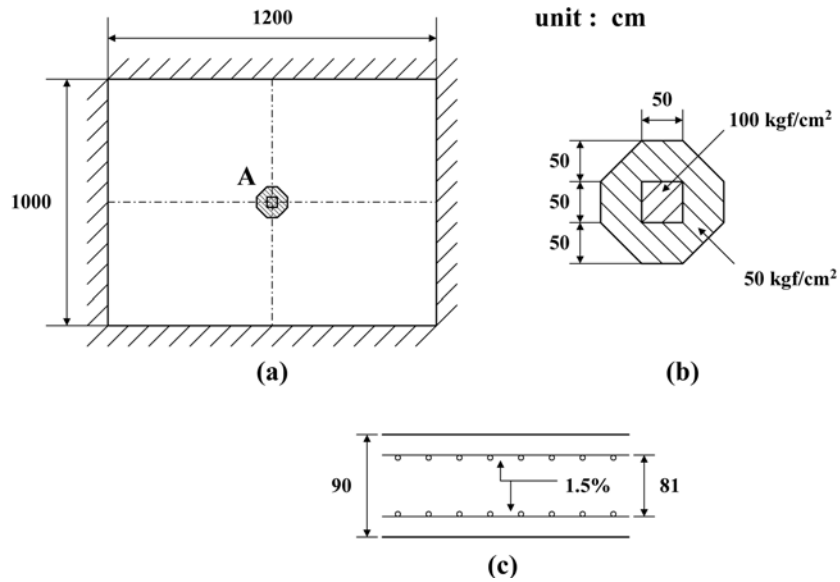


Fig. 7 Example of a reinforced concrete plate (Stangenberg 1974) (a) system, analyzed sector, (b) load distribution, (c) thickness and reinforcement details (1 kgf/cm² = 0.098 MPa)

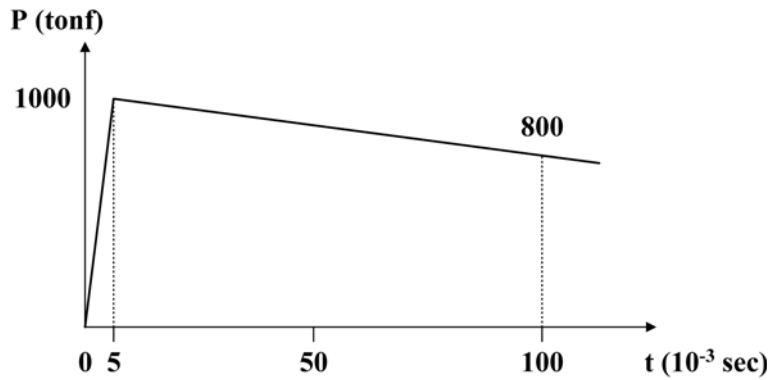


Fig. 8 Load time history for jet force (Stangenberg 1974) (1 tonf = 9.80665 kN)

Table 1 Material properties (Stangenberg 1974)

Concrete	E_c (kgf/cm ²)	340000
	f'_c (kgf/cm ²)	350.0
	f'_t (kgf/cm ²)	41.4
	ν	0.2
	ρ (kgf-sec ² /cm ⁴)	0.0000025
Steel	E_s (kgf/cm ²)	2100000
	f_y (kgf/cm ²)	4200

Note: 1 kgf/cm² = 0.098 MPa

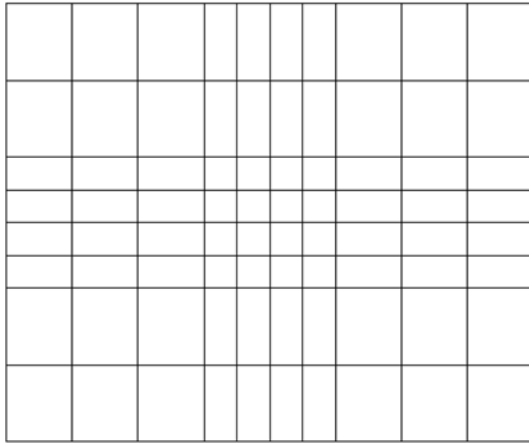


Fig. 9 Finite element mesh used for analysis

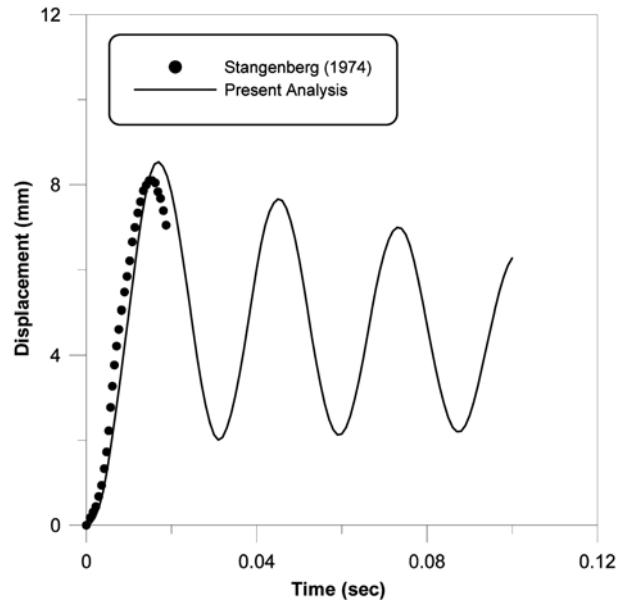


Fig. 10 Displacement-time history of reinforced concrete clamped plate subjected to central jet force

maximum deflection may be due to the differences in the material model used, discretization of plate, modeling of the pressure load (jet force) and approximation made in the numerical techniques used. Also, in the nonlinear response the deflection is considerably amplified, the period of vibration elongated and the amplitude of vibration diminished due to dissipation of energy, compared with that of the linear elastic case.

4.2 Dynamic response of reinforced concrete containment shell

The program was used to study the nonlinear dynamic response of a reinforced concrete nuclear secondary containment shell. The geometry of the containment shell is shown in Fig. 11. The built-in reinforced concrete shell under aircraft impact load was studied earlier by Reborá *et al.* (1976). The shell was composed of cylindrical and spherical parts of constant thickness. The reinforcement, placed circumferentially and meridionally on the interior and exterior surfaces, consisted of bars of diameter 40 mm, spaced at 80 mm, resulting in a percentage of reinforcement of 1.1%. The material properties used are shown in Table 2.

The horizontal impact of an aircraft on the shield building of a nuclear power plant was analyzed. A horizontal impact was assumed on an impact area 28 m² as shown in Fig. 11. The loading function is specified in Fig. 12.

A mesh of 90 shell elements was used in the analysis as shown in Fig. 13. The fundamental period of vibration (T) of the shell was 0.23 second. A time step of $\Delta t = 0.01$ second ($T/23$) was used for time step integration. Damping was neglected in the analysis, because it does not affect the maximum response from impulse-type loading (Clough 1975).

The results were obtained for a point "A" (see Fig. 11) near the junction of the cylindrical and spherical portions of the containment shell. For one point on the shell, the displacement was plotted

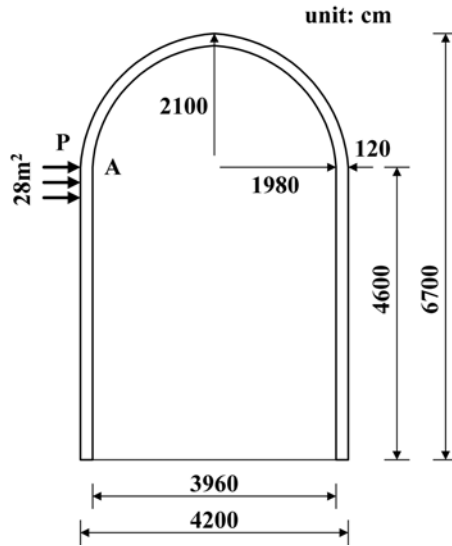


Fig. 11 Geometry of reinforced concrete nuclear containment shell (Rebora *et al.* 1976)

Table 2 Material properties (Rebora *et al.* 1976)

Concrete	E_c (kgf/cm ²)	369400
	f'_c (kgf/cm ²)	420.0
	f'_t (kgf/cm ²)	45.4
	ν	0.17
	ρ (kgf-sec ² /cm ⁴)	0.0000025
Steel	E_s (kgf/cm ²)	2100000
	f_y (kgf/cm ²)	4600

Note: 1 kgf/cm² = 0.098 MPa

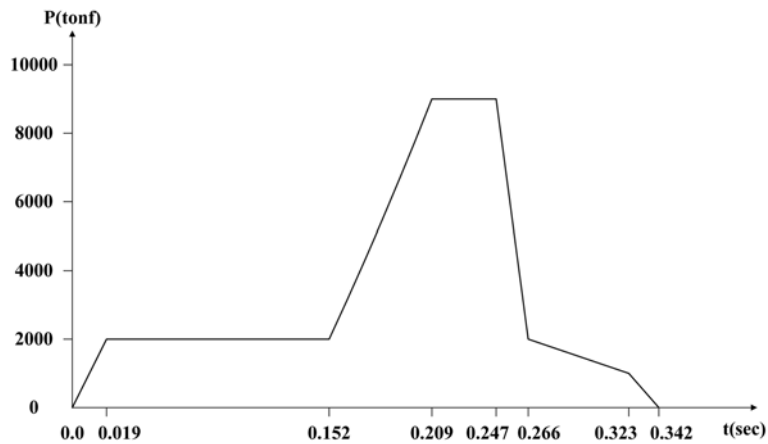


Fig. 12 Load time history for impact force (Rebora *et al.* 1976) (1 tonf = 9.80665 kN)

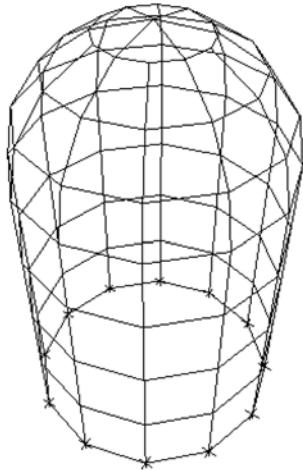


Fig. 13 Finite element mesh for reinforced concrete containment shell

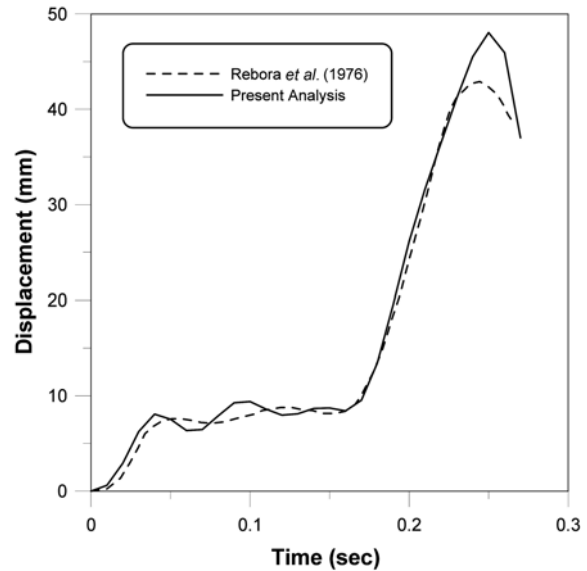


Fig. 14 Nonlinear displacement as function of time

for time steps as a function of time in Fig. 14. The agreement between the present analytical results and Rebora's results gave satisfactory agreement in terms of the predicted dynamic response.

4.3 Concrete containment vessel subjected to seismic loading

The dynamic response analysis of a prestressed concrete containment vessel (PCCV) was conducted and compared with experiments established as the benchmark test. The PCCV test model was subjected to various levels of acceleration input in the horizontal and vertical directions (Sandia National Laboratories 1999).

Fig. 15 shows the general layout. The test model had a cylindrical barrel with an inside diameter of 4.3 m, a wall thickness of 0.163 m, and a height of 3.43 m. It was cast on a 9 m square by 1 m thick basemat, which was rigidly and securely bolted to the shake table. The top cap is 1 m thick with weights bolted on the top and bottom surfaces and around the outer edge. Two buttresses ran the length of the cylinder for anchoring the hoop tendons. The direction of horizontal shaking was along the diametric line intersection the two buttresses. The basemat and supporting frames weighed about 260 metric tons, the cylindrical portion weighed 63 metric tons, and the upper section with the added mass weighed 474 metric tons.

The liner was 1.6 mm thick throughout most of the cylindrical region. The value of steel ratio (ρ) in the cylindrical section varied in the vertical direction from $\rho=1.7\%$ near the basemat to $\rho=0.9\%$ near the top. In the hoop direction, $\rho=2.5\%$ near the bottom of the cylindrical section, and $\rho=1.0\%$ near the top of the wall. Prestressing tendons were 12.7 mm diameter seven-wire strands in a plastic sheathing. The vertical tendons were spaced uniformly at 2.86 degree increments, while the hoop tendons were spaced uniformly at a distance of 130 mm. The material properties used in the model are summarized in Table 3.

Fig. 16 shows the response spectra for the horizontal and vertical components of the S1 and S2

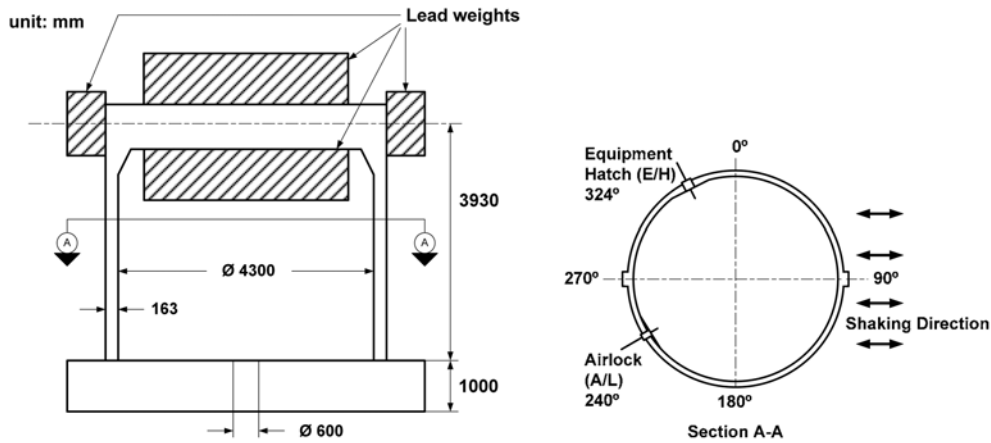


Fig. 15 Dimension of prestressed concrete containment vessel model (Sandia National Laboratories 1999)

Table 3 Material properties (Sandia National Laboratories 1999)

Concrete	E_c (MPa)	23438
	f'_c (MPa)	38.8
	ν	0.19
Rebar	E_s (MPa)	196133
	f_y (MPa)	432
Liner	E_s (MPa)	209862
	f_y (MPa)	202
Tendon	E_s (MPa)	194172
	f_y (MPa)	1314

target acceleration records (Sandia National Laboratories 1999). These spectral curves were generated from the time history records. Several sequential tests of S1 and S2 design-level earthquakes were also conducted.

A total of 289 layered shell elements and 47 unbonded tendon elements are used for the PCCV model, respectively. An unbonded tendon element based on the finite element method, that can represent the interaction between tendon and concrete, is used (Kim *et al.* 2008). The liner is modeled as fully bonded to the concrete and linear plasticity is included in the analysis. A schematic of the model is presented in Fig. 17.

Numerical and experimental natural frequencies were presented in Table 4, where the experimental ones were obtained from low-level random excitation. The Rayleigh damping corresponding to modal damping of 3% was used. The analytical results show good agreement with the experimental results.

The dynamic analysis used the direct integration method in the time domain. Hysteresis damping was explicitly considered through internal loops defined in constitutive relations. Structural viscous damping was not considered.

The relationship between maximum shear force and overall displacement is obtained as shown in

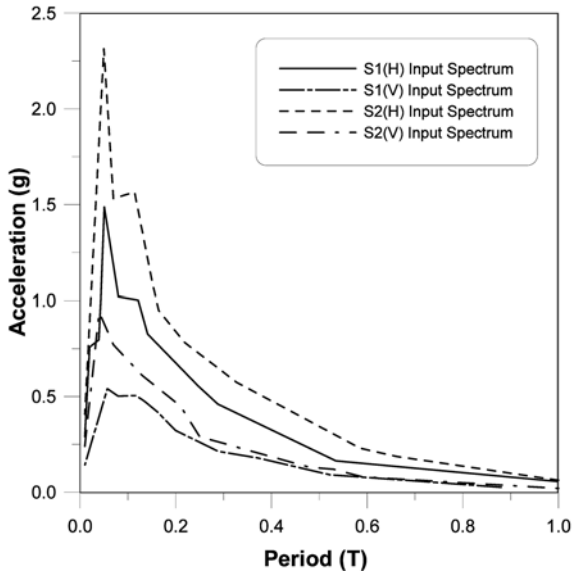


Fig. 16 Horizontal and vertical acceleration spectra for S1 and S2 target acceleration input (Sandia National Laboratories 1999)

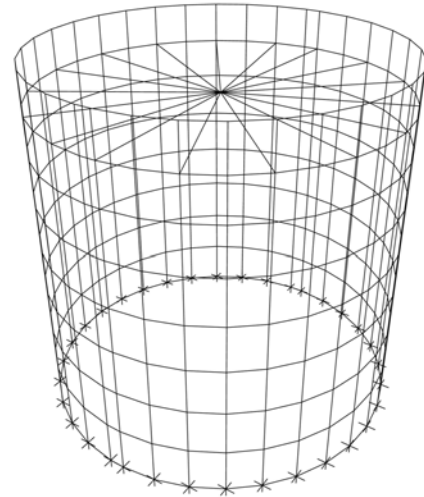


Fig. 17 Schematic of the nonlinear analytical model

Table 4 Measured and estimated natural frequencies of the structure (Hz)

Natural frequency	Experiment	Analysis	Ratio of experimental and analytical results
First mode	10.8	11.1	0.97

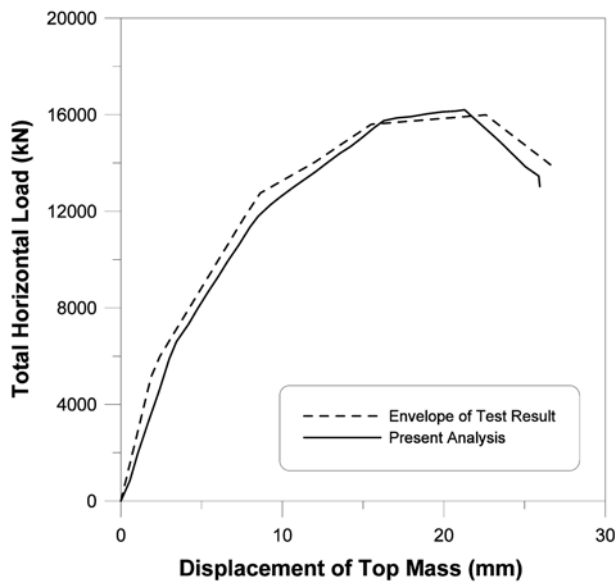


Fig. 18 Comparison of analysis and experimental results

Fig. 18. Fig. 19 shows the relationship between shear force and displacement at S2 shaking and collapse stage. The analytical solution has good agreement with the test results in linear behavior region as well as in nonlinear behavior region.

In general, the natural frequency of the structure tends to shift to lower when structural integrity starts to be deteriorated. Fig. 20, that shows the transition of the natural frequencies of the model, demonstrates this tendency. Table 5 summarizes the responses of the test model at major excitations. Analysis showed fair agreement with experiment in term of maximum response. The analysis verified the reasonable accuracy of the internal loops in the constitutive models.

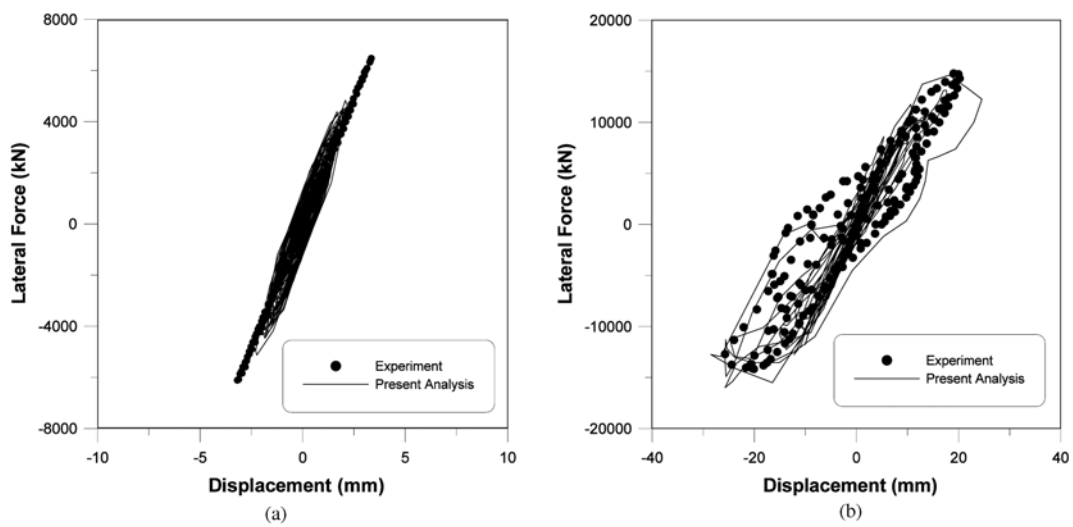


Fig. 19 Restoring force (a) S2, (b) collapse stage

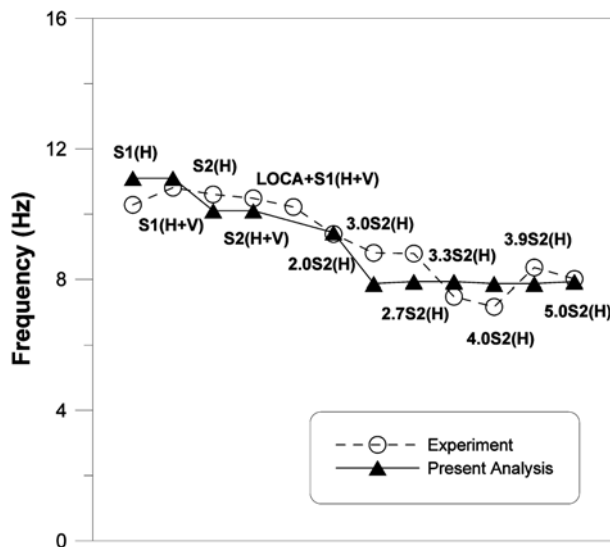


Fig. 20 Transition of the dominant natural frequency

Table 5 Maximum responses of test model

Shaking test name	Direction of excitation	Maximum input acceleration (Gal)	Maximum response at top slab			
			Experiment		Analysis	
			Acceleration (Gal)	Displacement (mm)	Acceleration (Gal)	Displacement (mm)
S1(H)	Horizontal	354	981	2.20	1080	2.42
S1(H+V)	Horizontal	299	1162	2.78	1031	2.23
	Vertical	139	347	0.08	370	0.05
S2(H)	Horizontal	419	1362	3.34	823	1.88
S2(H+V)	Horizontal	441	1529	3.94	928	2.21
	Vertical	226	786	0.17	543	0.14
LOCA+	Horizontal	289	1012	2.73	835	1.87
S1(H+V)	Vertical	157	600	0.16	319	0.14
2.0S2(H)	Horizontal	1414	2650	12.60	2540	7.67
3.0S2(H)	Horizontal	2680	3300	19.60	4613	15.80
2.7S2(H)	Horizontal	2500	3030	18.43	4153	14.90
3.3S2(H)	Horizontal	2510	3010	18.32	4173	15.10
4.0S2(H)	Horizontal	2970	3340	21.90	4315	16.70
3.9S2(H)	Horizontal	2510	2980	20.20	3832	14.90
5.0S2(H)	Horizontal	3280	3120	26.00	4456	22.60

5. Conclusions

A formulation was presented for the nonlinear dynamic analysis of reinforced concrete shell structures. Such a formulation was based on the four-node quadrilateral flat shell element with drilling rotational stiffness.

To analyze the reinforced concrete shell structures with nonlinear dynamic behavior, this study introduced the layer method, which assumes that several thin plane stress elements are layered in the direction of thickness. The analysis accounted for material nonlinearity by incorporating tensile, compressive and shear models of cracked concrete, as well as a model for the reinforcing steel. The low-cycle fatigue of both concrete and reinforcing bars has been taken into account to predict a reliable dynamic behavior. Thus, the developed element predicts with reasonable accuracy the behavior of reinforced concrete shell structures subjected to dynamic loading.

The numerical model was applied to three examples, and they were analyzed. Their results were compared with experimental and analytical results from other researchers. A comparison of these results with test data confirmed that the numerical model can give good predictions for dynamic responses of reinforced concrete shell structures. Hence, nonlinear finite element analysis would be a useful tool for investigating design details or the dynamic response of reinforced concrete shell structures.

Finally, nonlinear finite element procedure should be carried out on important reinforced concrete

structures such as nuclear containment shells to simulate the actual performance of the structures under design dynamic loads. Future work will include a formulation of out-of-plane shear and geometrical nonlinearity for reinforced concrete shell elements.

Acknowledgements

This research was supported by a grant(code#06-E01) from Virtual Construction Research Center Program funded by Ministry of Land, Transport and Maritime Affairs of Korean government. The authors wish to express their gratitude for the support received.

References

- ACI (2001), *Finite Element Analysis of Reinforced Concrete Structures*, Farmington Hills, MI.
- ASCE (1993), "Finite element analysis of reinforced concrete structures", *Proceedings of the International Workshop*, New York, June.
- ASCE (2001), *Modeling of Inelastic Behavior of RC Structures Under Seismic Loads*, ASCE, Reston.
- Clough, W. and Penzien, J. (1975), *Dynamic of Structures*, McGraw-Hill, New York.
- Hughes, T.J.R. (2000), *The Finite Element Method*, Prentice-Hall.
- Kakuta, Y., Okamura, H. and Kohno, M. (1982), "New concepts for concrete fatigue design procedures in Japan", IABSE Colloquium of Fatigue of Steel and Concrete Structures, Lausanne.
- Kato, B. (1979), "Mechanical properties of steel under load cycles idealizing seismic action", *CEB Bull.*, **13**(1), 7-27.
- Kim, T.H., Kim, B.S., Chung, Y.S. and Shin, H.M. (2006), "Seismic performance assessment of reinforced concrete bridge piers with lap splices", *Eng. Struct.*, **28**(6), 935-945.
- Kim, T.H., Lee, K.M., Chung, Y.S. and Shin, H.M. (2005), "Seismic damage assessment of reinforced concrete bridge columns", *Eng. Struct.*, **27**(4), 576-592.
- Kim, T.H., Lee, K.M. and Shin, H.M. (2002), "Nonlinear analysis of reinforced concrete shells using layered elements with drilling degree of freedom", *ACI Struct. J.*, **99**(4), 418-426.
- Kim, T.H., Lee, K.M., Yoon, C.Y. and Shin, H.M. (2003), "Inelastic behavior and ductility capacity of reinforced concrete bridge piers under earthquake: Theory and formulation", *J. Struct. Eng-ASCE*, **129**(9), 1199-1207.
- Kim, T.H., Park, J.G., Kim, Y.J. and Shin, H.M. (2008), "A computational platform for seismic performance assessment of reinforced concrete bridge piers with unbonded reinforcing or prestressing bars", *Comput. Concrete*, **5**(2), 135-154.
- Kim, T.H. and Shin, H.M. (2001), "Analytical approach to evaluate the inelastic behaviors of reinforced concrete structures under seismic loads", *J. Earthq. Eng. Soc. Korea*, **5**(2), 113-124.
- Li, B., Maekawa, K. and Okamura, H. (1989), "Contact density model for stress transfer across cracks in concrete", *J. facult. Eng., Univ. Tokyo*, **40**(1), 9-52.
- Maekawa, K. and Okamura, H. (1983), "The deformational behavior and constitutive equation of concrete using elasto-plastic and fracture model", *J. facult. Eng., Univ. Tokyo*, **37**(2), 253-328.
- Mander, J.B., Panthaki, F.D. and Kasalanati, K. (1994), "Low-cycle fatigue behavior of reinforcing steel", *J. Mater. Civil Eng.*, **6**(4), 453-468.
- Miner, M.A. (1945), "Cumulative damage in fatigue", *J. Appl. Mech.*, **67**, 159-164.
- Rebora, B., Zimmermann, T. and Wolf, J.P. (1976), "Dynamic rupture analysis of reinforced concrete shells", *Nucl. Eng. Des.*, **37**, 269-297.
- Sandia National Laboratories (1999), Seismic Analysis of a Prestressed Concrete Containment Vessel Model, NUREG/CR-6639.
- Semblat, J.F., Aouameur, A. and Ulm, F.J. (2004), "Non linear seismic response of a low reinforced concrete structure : modeling by multilayered finite shell elements", *Struct. Eng. Mech.*, **18**(2), 211-229.

- Shima, H., Chou, L. and Okamura, H. (1987), "Micro and macro models for bond behavior in reinforced concrete", *J. Facult. Eng., Univ. Tokyo*, **39**(2), 133-194.
- Stangenberg, F. (1974), "Nonlinear dynamic analysis of reinforced concrete structures", *Nucl. Eng. Des.*, **29**, 71-88.
- Taylor, R.L. (2000), *FEAP - A Finite Element Analysis Program* (Version 7.2), Users manual, Vols. 1-2.